Archives of Cardiovascular Disease (2016) 109, 104—112

View metadata, citation and similar papers at core.ac.uk

brought to you by CORE

provided by Elsevier - Publisher Connector

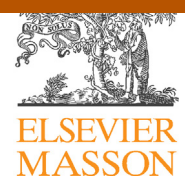

Available online at ScienceDirect www.sciencedirect.com

Elsevier Masson France EM|consulte www.em-consulte.com/en

CLINICAL RESEARCH

Speckle-tracking imaging in patients with Eisenmenger syndrome

Speckle-tracking *et syndrome d'Eisenmenger*

Pamela Moceri[a,b,*], Xavier Iriart[c], Priscille Bouvier[a], Delphine Baudouy[a,b], Pierre Gibelin[a,b], Redouane Saady[a,b], Jeremy Laïk[a], Pierre Cerboni[a], Jean-Benoit Thambo[c], Emile Ferrari[a,b]

[a] *Cardiology Department, hôpital Pasteur, CHU de Nice, 06002 Nice, France*
[b] *Faculté de médecine, université de Nice Sophia-Antipolis, 06002 Nice, France*
[c] *Cardiology Department, hôpital Haut-Lêveque, CHU de Bordeaux, 33600 Bordeaux, France*

Received 24 September 2015; received in revised form 18 November 2015; accepted 21 November 2015
Available online 8 February 2016

KEYWORDS
Congenital heart defects;
Pulmonary hypertension;
Eisenmenger syndrome;
Echocardiography;
Speckle-tracking imaging

Summary
Background. — Adults with Eisenmenger syndrome have a survival advantage over those with idiopathic pulmonary arterial hypertension. Improved survival may result from preservation of right ventricular (RV) function.
Aims. — To assess left ventricular (LV) and RV remodelling in patients with Eisenmenger syndrome compared to a control population, using speckle-tracking imaging.
Methods. — Adults with Eisenmenger syndrome and healthy controls were enrolled into this prospective two-centre study. Patients with Eisenmenger syndrome with low acoustic windows, irregular heart rhythm or complex congenital heart disease were excluded. Clinical assessment, B-type natriuretic peptide (BNP), 6-minute walk test and echocardiography (including dedicated views to perform offline two-dimensional-speckle-tracking analysis) were performed on inclusion.

Abbreviations: 2D, two-dimensional; BNP, B-type natriuretic peptide; DICOM, Digital Imaging and Communications in Medicine; DVD, digital video disc; LV, left ventricular; NYHA, New York Heart Association; PAH, pulmonary artery hypertension; RV, right ventricular; SD, standard deviation; TAPSE, tricuspid annular plane systolic excursion.

* Corresponding author. Hôpital Pasteur, CHU de Nice, service de cardiologie, avenue de la Voie-Romaine, 06002 Nice, France.
E-mail address: moceri.p@chu-nice.fr (P. Moceri).

http://dx.doi.org/10.1016/j.acvd.2015.11.013
1875-2136/© 2015 Elsevier Masson SAS. All rights reserved.

Results. — Our patient population ($n = 37$; mean age 42.3 ± 17 years) was mostly composed of patients with ventricular septal defect (37.8%) or atrial septal defect (35.1%). Compared with the control population ($n = 30$), patients with Eisenmenger syndrome had reduced global LV longitudinal strain (-17.4 ± 3.5 vs. -22.4 ± 2.3; $P < 0.001$), RV free-wall longitudinal strain (-15.0 ± 4.7 vs. -29.9 ± 6.8; $P < 0.001$) and RV transverse strain (25.8 ± 25.0 vs. 44.5 ± 15.1; $P < 0.001$). Patients with Eisenmenger syndrome also more frequently presented a predominant apical longitudinal and transverse strain profile. Among patients with Eisenmenger syndrome, those with a post-tricuspid shunt presented with reduced global LV longitudinal strain but increased RV transverse strain, compared to patients with pre-tricuspid shunt.
Conclusion. — Patients with Eisenmenger syndrome had impaired longitudinal RV and LV strain, but present a relatively important apical deformation. RV and LV remodelling, as assessed by speckle-tracking imaging, differ between patients with pre- and post-tricuspid shunt.
© 2015 Elsevier Masson SAS. All rights reserved.

MOTS CLÉS
Cardiopathies congénitales ;
Hypertension pulmonaire ;
Syndrome d'Eisenmenger ;
Échocardiographie ;
Speckle-tracking imaging

Résumé
Contexte. — Les patients avec syndrome d'Eisenmenger présentent un avantage de survie par rapport aux patients avec hypertension artérielle pulmonaire non liée aux cardiopathies congénitales. La préservation de la fonction ventriculaire droite (VD) pourrait expliquer cet avantage.
Objectifs. — D'étudier le remodelage ventriculaire droit et gauche (VG) à l'aide du « speckle-tracking imaging » chez les patients avec syndrome d'Eisenmenger.
Méthodes. — Nous avons inclus de façon prospective patients avec syndrome d'Eisenmenger et des patients témoins au sein d'une étude bicentrique. Les patients atteints d'un syndrome d'Eisenmenger lié à une cardiopathie congénitale complexe, peu échogènes ou en arythmie ont été exclus.
Résultats. — Notre population de syndrome d'Eisenmenger ($n = 37$; âge moyen $42,3 \pm 17$ années) se compose majoritairement de patients avec communication inter-ventriculaire (37,8 %) et inter-atriale (35,1 %). Comparativement à la population témoin ($n = 30$), les patients présentent une réduction du strain global longitudinal VG ($-17,4 \pm 3,5$ vs $-22,4 \pm 2,3$; $p < 0,001$), du strain longitudinal ($-15,0 \pm 4,7$ vs $-29,9 \pm 6,8$; $p < 0,001$) et transverse VD ($25,8 \pm 25,0$ vs $44,5 \pm 15,1$; $p < 0,001$). Ils présentent également de façon plus fréquente un profil de déformation apicale important. Au sein de la population avec syndrome d'Eisenmenger, les patients avec shunt post-tricuspide ont un strain longitudinal VG réduit tandis que leur strain transverse VD est meilleur par rapport aux patients avec shunt pré-tricuspide.
Conclusion. — Les patients avec syndrome d'Eisenmenger présentent une altération du strain longitudinal VD et VG, mais un profil de déformation VD avec déformation apicale prédominante. Le remodelage VD et VG évalué par la technique du *speckle-tracking* a aussi permis de constater des différences dans la population syndrome d'Eisenmenger en fonction de la localisation du shunt pré- ou post-tricuspide.
© 2015 Elsevier Masson SAS. Tous droits réservés.

Introduction

Pulmonary hypertension is a severe disorder defined as an increase in mean pulmonary arterial pressure > 25 mmHg at rest [1]. Patients with pulmonary hypertension can be divided into subgroups sharing similar underlying pathophysiology [2]. Eisenmenger syndrome is the most advanced form of pulmonary artery hypertension (PAH) associated with congenital heart disease. Patients with Eisenmenger syndrome have a survival advantage over those with other causes of PAH [3]. Survival and symptoms are closely related to right ventricular (RV) function and adaptation [4—8]. Improved survival may result from preservation of RV function, as the right ventricle may not undergo 'normal' remodelling at birth and sustain raised pulmonary vascular resistance. Differences within the spectrum of Eisenmenger syndrome have already been described, especially between patients with pre- and post-tricuspid shunt [9]. Thus, we hypothesize that different cardiac remodelling might explain the differences observed between patients with pre- and post-tricuspid shunt.

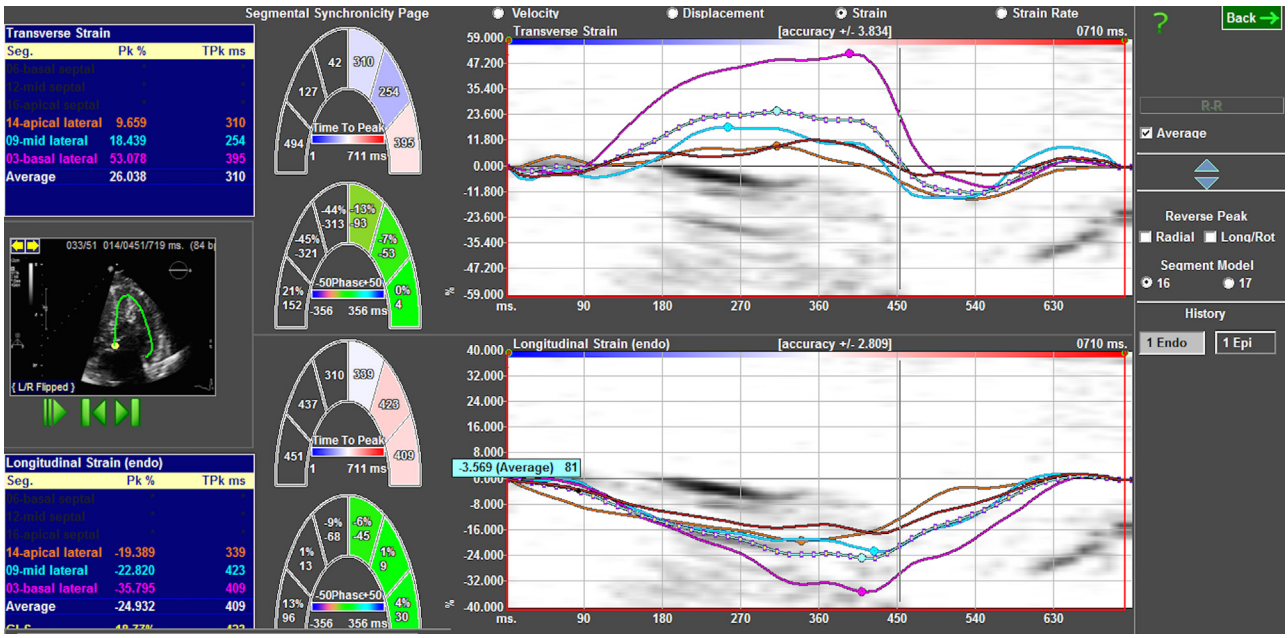

Figure 1. Example of right ventricular speckle-tracking analysis using TomTec (TomTec Imaging Systems GmbH, Germany).

Speckle-tracking imaging is a relatively recent tool used to investigate RV and left ventricular (LV) functions, especially in the setting of pulmonary hypertension [10]. Speckle-tracking imaging has been related to cardiovascular events and mortality in patients with pulmonary hypertension [11—13]; however, little is known about the role of speckle-tracking imaging in Eisenmenger syndrome.

The aim of our study was to identify LV and RV remodelling differences in patients with Eisenmenger syndrome compared to healthy controls, using speckle-tracking imaging. We also aimed to describe LV and RV remodelling differences between patients with pre- and post-tricuspid shunt.

Methods

Study design and patients

We performed a prospective two-centre case-control study on patients with Eisenmenger syndrome who were followed up at our centres (Pasteur University Hospital, Nice, France and Haut-Leveque University Hospital, Bordeaux, France) between September 2012 and June 2015.

Adults with Eisenmenger syndrome were included in the study. Patients with low acoustic windows, irregular heart rhythm or complex congenital heart disease (e.g. univentricular heart and systemic right ventricle) were excluded from this study to standardize the interpretation of echocardiographic data. Demographic and clinical data (age, sex, diagnosis, New York Heart Association [NYHA] class, heart rate, specific advanced therapy), B-type natriuretic peptide (BNP) plasma concentrations and 6-minute walk test distance were collected on inclusion (at the time of echocardiography).

Adult healthy controls were enrolled either in the outpatient clinic or from hospital employees and fellows in training. All underwent echocardiography examination and none were competitive athletes. Criteria for recruitment included age $\geq$ 18 years, no history or symptoms of cardiovascular or lung disease, no ongoing or previous cardio- or vasoactive treatment, and normal results on electrocardiogram (ECG) and physical examinations. Exclusion criteria included tricuspid regurgitation more than mild, poor acoustic window, pregnancy and obesity.

All study subjects gave informed consent to participate in the study. Our local ethics committee approved the study protocol.

Echocardiographic measurements

Echocardiographic examination was performed using an IE-33 (Philips Medical system, Andover, MA, USA) or a Vivid 7 ultrasound system (General Electric Healthcare, Milwaukee, WI, USA). Doppler echocardiography was performed according to the recommendations of the American Society of Echocardiography [14—16]. The ratio of RV wall thickness to RV diameter was calculated to distinguish between more concentric and eccentric hypertrophy.

RV myocardial strain was studied using speckle-tracking echocardiography of the apical long axis, obtained from the apical four-chamber view during a quiet breath hold with a frame rate of 55—75/s (Fig. 1). LV myocardial global longitudinal strain was assessed using speckle-tracking echocardiography of the apical long axis, obtained from apical four-, three- and two-chamber views of the left ventricle. LV circumferential strain was obtained by analysing the parasternal short axis of the LV mid-cavity.

Two consecutive heart cycles were recorded and averaged (excluding premature beats). The offline analysis was performed using commercially available semiautomated two-dimensional (2D) strain software: Tomtec Cardiac Performance Analysis (TomTec Imaging Systems GmbH, Germany) for longitudinal, transverse and circumferential

strain analysis. The peak RV free-wall longitudinal strain was defined as the peak negative value on the strain curve; peak RV free-wall transverse strain was defined as the peak positive value on the strain curve before pulmonary valve closure. The RV cavity was traced manually, delineating a region of interest composed of three segments of the lateral wall: basal, mid-cavity and apical. After segmental tracking, the RV longitudinal and transverse curves were generated and the average values of longitudinal and transverse strain calculated. A predominant apical deformation pattern was defined by an apical peak strain value above the peak strain value of the median and basal segments. The Eisenmenger echocardiographic prognostic score has been calculated for each patient [7].

Ultrasound scanning was performed in both centres. The physician performing the ultrasound for a clinical purpose interpreted the echocardiography immediately. Images were then stored on a hard drive or digital videodisc (DVD) in native Digital Imaging and Communications in Medicine (DICOM) format. Images from Bordeaux were sent electronically or via mail (DVDs) to Nice. One staff cardiologist with advanced training in echocardiography interpreted 2D echo datasets and performed the offline speckle-tracking analysis. In a subset of 20 controls, included and scanned in Nice, intra-operator variability was assessed for RV longitudinal and transverse strain reproducibility.

Statistical analysis

Data are summarized as mean ± standard deviation (SD) for continuous variables and number (%) for categorical variables. Normally distributed variables were tested by a two-tailed Student's *t*-test for unpaired data. Variables that were not normally distributed were tested by the Mann—Whitney *U*-test. Categorical variables were compared using Fisher's exact test. Variability was assessed, with good agreement defined as > 0.80, using intra-class correlation analysis. Given the rarity of the disease, no sample size calculation was possible, hence consecutive patients were included according to the capabilities of our centres.

For all analyses, statistical significance was defined as $P < 0.05$. Statistical analyses were performed using MedCalc 15.8 for Windows (MedCalc Software, Ostend, Belgium).

Results

General characteristics of the population

A total of 37 consecutive patients with Eisenmenger syndrome (mean age 42.3 ± 17 years; 73.0% female) and 30 healthy controls (mean age 33.8 ± 11 years; 66.7% female) were included in this study. The underlying congenital heart defect was ventricular septal defect in 14 patients (37.8%), atrial septal defect in 13 (35.1%) patients, complete atrioventricular septal defect in seven (18.9%) patients and patent ductus arteriosus in 3 (8.1%) patients. Patient characteristics are detailed in Table 1.

Regarding standard echocardiographic characteristics, patients with Eisenmenger syndrome had overall dilated right hearts (both atria and ventricles), and mean RV fractional area changes and tricuspid annular plane systolic excursion (TAPSE) were lower than normal established values. Standard echocardiographic characteristics of our patient population are described in Table 2.

Table 1 General characteristics of the patient population.

	Eisenmenger syndrome ($n = 37$)
Age (years)	42.3 ± 17
Women	27 (73.0)
NYHA class III/IV	20 (54.1)
Resting O_2 saturation (%)	88.6 ± 5
B-type natriuretic peptide (ng/L)	165.1 ± 224
6-minute walk distance (m)	345.5 ± 109
Advanced therapy at baseline	29 (78.4)
Death or hospitalization	10 (27.0)

Data are expressed as mean ± standard deviation or number (%). NYHA: New York Heart Association.

Speckle-tracking imaging: comparison of Eisenmenger vs. controls

Differences in myocardial deformation between patients with Eisenmenger syndrome and the control population are presented in Table 3 and Fig. 2. Compared with the control healthy population, patients with Eisenmenger syndrome had reduced global LV longitudinal strain but similar LV circumferential strain. The RV free-wall longitudinal and transverse strains were both markedly reduced compared with controls ($P < 0.001$). The healthy population presented a decreasing RV strain gradient from the base to the apex. Conversely, patients with Eisenmenger syndrome more often presented with a predominant apical deformation profile, as assessed by longitudinal and transverse RV strain.

Longitudinal RV free-wall strain was significantly correlated ($r = 0.6$; $P = 0.007$) with the Eisenmenger echocardiographic prognostic score [7], but not with RV transverse strain, nor LV circumferential or longitudinal strain.

Differences between patients with pre- and post-tricuspid shunt

Increased RV wall thickness and increased RV wall thickness/inlet diameter ratio were found in patients with post-tricuspid shunt (Table 2), suggesting more concentric hypertrophy in these patients. Increased RV outflow tract velocity-time integral (VTI) was also observed, suggesting preserved pulmonary output in patients with post-tricuspid shunt. A trend towards reduced RV systolic function, as assessed by the fractional area change, was noted in patients with pre-tricuspid shunt.

Speckle-tracking analysis also highlighted differences between patients with pre- and post-tricuspid shunt (Table 4 and Fig. 3): LV longitudinal strain was lower in patients with post-tricuspid shunt ($P = 0.04$) whereas LV circumferential

Table 2 Standard echocardiographic characteristics—differences between pre- and post-tricuspid shunt patients.

	Total population ($n=37$)	Pre-tricuspid shunt ($n=13$)	Post-tricuspid shunt ($n=24$)	P
RA area (cm^2)	24.5 ± 9	27.2 ± 10	22.7 ± 8	0.19
RA/LA area ratio	1.45 ± 0.4	1.32 ± 0.3	1.53 ± 0.4	0.17
RA pressure (mmHg)	10.0 ± 3.2	11.1 ± 3.3	8.6 ± 2.3	0.10
RV inlet (mm)	46.5 ± 8	48.9 ± 9	44.5 ± 6	0.10
RV wall thickness (mm)	11.8 ± 3.0	9.6 ± 2.4	13.6 ± 2.2	< 0.001
RV wall/diameter ratio	0.26 ± 0.09	0.19 ± 0.05	0.32 ± 0.07	< 0.001
TAPSE (mm)	18.8 ± 5.9	21.5 ± 6.3	17.4 ± 5.4	0.08
TV s′ (cm/s)	9.9 ± 2.7	10.5 ± 3.2	9.6 ± 2.4	0.41
RV FAC (%)	36.9 ± 10	32.0 ± 10	40.1 ± 8	0.09
IVA/$\sqrt{}$RR^2 (m/s^2)	2.2 ± 0.9	2.4 ± 1.3	2.4 ± 0.8	0.96
RV OT VTI (cm)	16.6 ± 5.8	13.8 ± 2.2	18.6 ± 6.8	0.05
PV acceleration time (ms)	68.6 ± 21	67.0 ± 18	70.0 ± 24	0.92
Tei index	0.68 ± 0.3	0.69 ± 0.3	0.67 ± 0.2	0.90
S/D ratio	1.07 ± 0.6	1.32 ± 0.8	0.84 ± 0.2	0.49
TV E/A	1.07 ± 0.6	0.90 ± 0.4	1.18 ± 0.7	0.50
TV E/e′	5.5 ± 3.1	4.0 ± 1.0	6.7 ± 3.7	0.06
TV e′ (cm/s)	9.4 ± 3.6	10.4 ± 2.9	8.7 ± 4.0	0.34
RV-RA gradient (mmHg)	95.7 ± 25	87.3 ± 29	102.4 ± 21	0.21
LV EF (%)	63.1 ± 14	67.1 ± 14	59.5 ± 14	0.21
LV EDD (mm)	41.9 ± 7.4	40.1 ± 7.0	43.7 ± 7.7	0.27
LA area (cm^2)	17.3 ± 6.9	20.1 ± 5.8	15.6 ± 7.0	0.04
MV E/A	1.2 ± 0.6	1.0 ± 0.4	1.4 ± 0.7	0.29
MV E/e′	6.8 ± 3.2	7.7 ± 4.1	6.2 ± 2.2	0.50
MV e′ (cm/s)	10.4 ± 4.0	10.7 ± 4.8	10.2 ± 3.5	0.84
LV diastolic eccentricity index	1.58 ± 0.3	1.63 ± 0.2	1.55 ± 0.3	0.46
Pericardial effusion	3 (8.1)	2 (15.4)	1 (4.2)	0.55

Data are expressed as mean ± standard deviation or number (%). e′: early diastolic tissue Doppler imaging velocity; E/A: ratio of early to late filling velocities; E/e′: ratio of early Doppler velocity to early diastolic tissue Doppler imaging velocity; EDD: end diastolic diameter; EF: ejection fraction; FAC: fractional area change; IVA: isovolumetric acceleration; LA: left atrial; LV: left ventricular; MV: mitral valve; OT: outflow tract; PV: pulmonary valve; RA: right atrial; RV: right ventricular; S/D ratio: systolic/diastolic duration ratio; TAPSE: tricuspid annular plane systolic excursion; TV: tricuspid valve; VTI: velocity-time integral.

Table 3 Myocardial deformation differences between patients with Eisenmenger syndrome and controls.

	Eisenmenger syndrome ($n=37$)	Control population ($n=30$)	P
Global LV longitudinal strain (%)	−17.4 ± 3.5	−22.4 ± 2.3	< 0.001
LV circumferential strain (%)	−22.7 ± 7.3	−21.9 ± 2.8	0.48
RV free-wall longitudinal strain (%)	−15.0 ± 4.7	−29.9 ± 6.8	< 0.001
Predominant apical RV longitudinal strain	27 (73.0)	3 (10.0)	< 0.001
RV free-wall transverse strain (%)	25.8 ± 25.0	44.5 ± 15.1	< 0.001
Predominant apical RV transverse strain	13 (35.1)	2 (6.7)	0.04

Data are expressed as mean ± standard deviation or number (%). LV: left ventricular; RV: right ventricular.

strain was similar in both groups. No difference in longitudinal RV strain was observed, although transverse RV strain was higher in patients with post-tricuspid shunt ($P=0.02$). There was no difference in the apical involvement in the RV deformation (longitudinal and transverse) between patients with pre- and post-tricuspid shunt.

Feasibility of speckle-tracking imaging

Intra-class correlation coefficients for intra-operator variability were 0.94 (95% confidence interval 0.87—0.97) and 0.92 (95% confidence interval 0.82—0.96) for longitudinal and transverse RV strain, respectively.

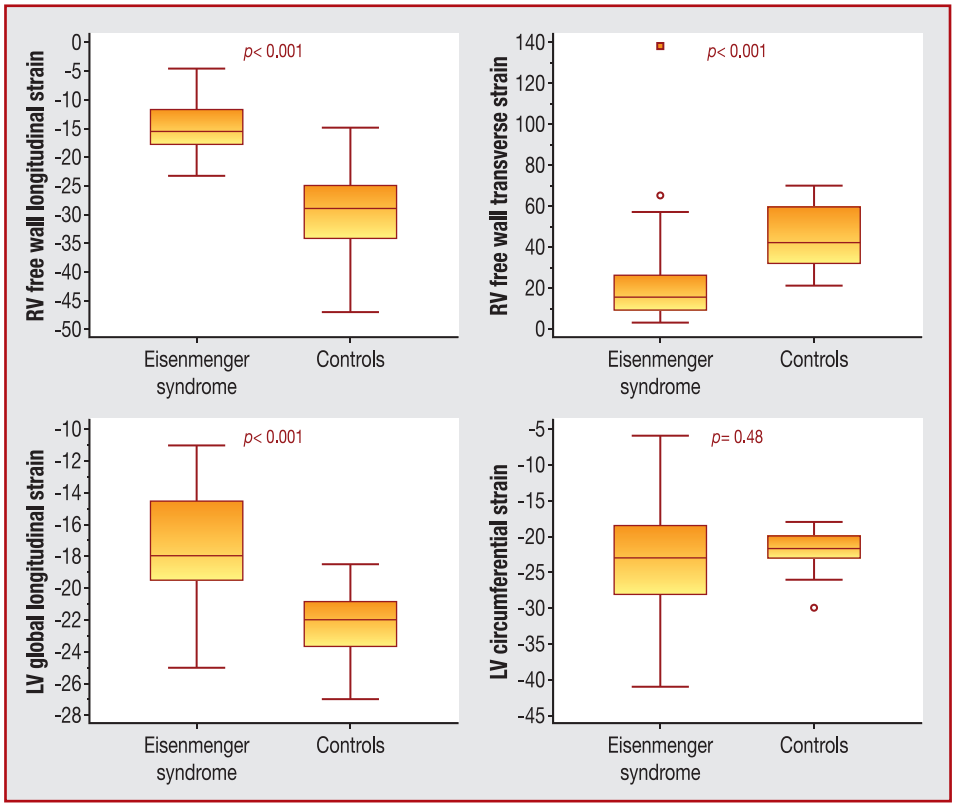

Figure 2. Differences in RV and LV myocardial deformation between the control population and Eisenmenger syndrome patients.

Table 4 Myocardial deformation differences between patients with pre- and post-tricuspid shunt.

	Pre-tricuspid shunt ($n = 13$)	Post-tricuspid shunt ($n = 24$)	*P*
Global LV longitudinal strain (%)	−19.3 ± 3.7	−16.5 ± 3.2	0.04
LV circumferential strain (%)	−23.2 ± 6.7	−22.5 ± 7.8	0.80
RV free-wall longitudinal strain (%)	−14.3 ± 6.2	−15.1 ± 3.6	0.62
Predominant apical RV longitudinal strain	9 (69.2)	18 (75.0)	0.98
RV free-wall transverse strain (%)	14.0 ± 8.5	32.2 ± 29.0	0.02
Predominant apical RV transverse strain	2 (15.4)	11 (45.8)	0.10

Data are expressed as mean ± standard deviation or number (%). LV: left ventricular; RV: right ventricular.

Discussion

Our study highlights differences in LV and RV remodelling between patients with Eisenmenger syndrome and controls: patients with Eisenmenger syndrome had impaired longitudinal and transverse RV strain as well as impaired LV longitudinal strain. Furthermore, our results show that in the group with Eisenmenger syndrome, patients with post-tricuspid shunt had impaired global LV longitudinal strain but increased RV free-wall transverse strain compared to patients with pre-tricuspid shunt.

The decline in RV function over time with pulmonary hypertension has been well described, however, only limited data are available regarding LV function. It was recently suggested that LV strain is associated with increased mortality in PAH [17]. Our study shows that LV mechanics are also affected in Eisenmenger syndrome, especially in patients with post-tricuspid shunt. Our results suggest that beyond the classic RV–LV interaction assessed by the LV eccentricity index, there is a direct effect of the prolonged elevation of RV after load in patients with post-tricuspid shunt. In these patients, the left ventricle is both ejecting into the aorta and participating in pulmonary output (given that the LV eccentricity index was similar in patients with pre- and post-tricuspid shunt in our study). Furthermore, in a large cohort study, LV eccentricity index was reported to be even lower in patients with post-tricuspid shunt compared to those with pre-tricuspid shunt [9], thus the alteration in LV longitudinal strain suggests a deeper involvement of the left ventricle in this disease. This could be explained by at least two hypotheses:

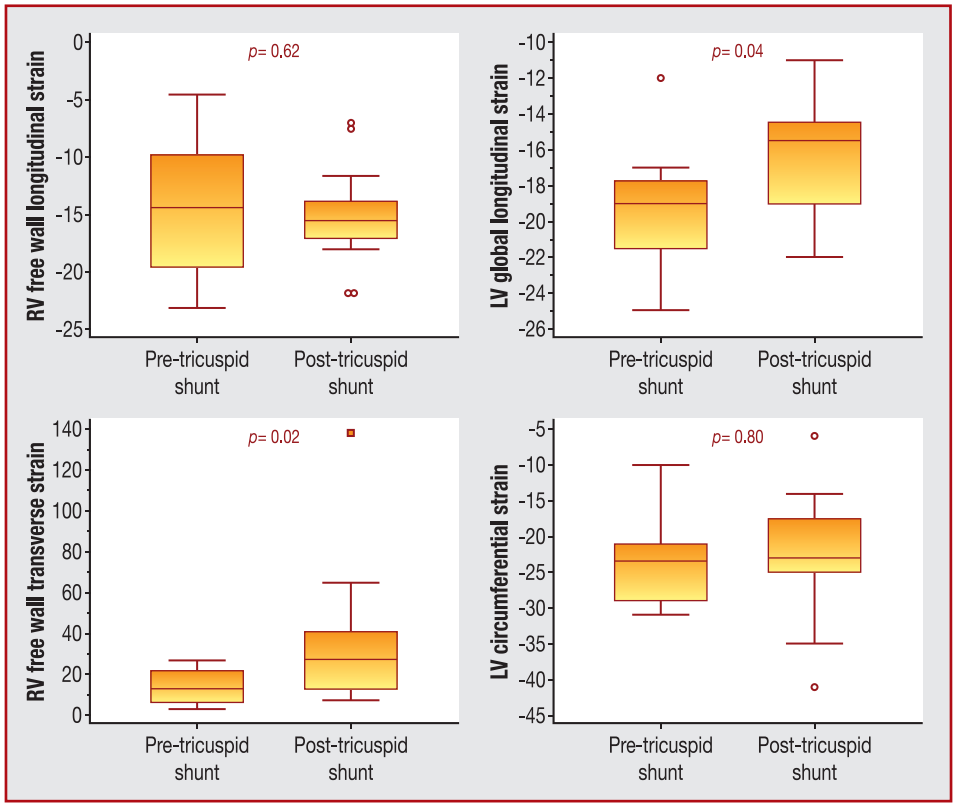

Figure 3. Differences in RV and LV myocardial deformation between pre- and post-tricuspid shunt patients.

- an increased mechanical stress (the left and right ventricle working together to eject into the aorta and pulmonary artery) in patients with ventricular septal defect;
- the effect of cyanosis (more profound in patients with post-tricuspid shunt) potentially inducing or increasing LV ischaemia.

The lack of correlation between the Eisenmenger echocardiographic prognostic score and transverse RV strain is not surprising, given that this score includes TAPSE, which assesses mostly longitudinal RV function (rationale for the correlation between TAPSE and RV longitudinal strain).

Despite the classic notion of 'preserved' RV function in patients with Eisenmenger syndrome [18], RV longitudinal and transverse strain were reduced compared to our control population. This finding supports the role of RV function in patients with Eisenmenger syndrome [7,19]. The concept of maintained RV function should probably only be used when comparing patients with PAH to those with congenital heart disease and PAH [3,20]. Patients with post-tricuspid shunt have a trend towards greater RV function compared to those with pre-tricuspid shut — as assessed by RV fractional area change — but similar TAPSE, despite the prolonged course of the disease in such patients. Increased RV transverse strain is consistent with a different RV remodelling over time in patients with post-tricuspid shunt, with increased transverse strain compensating for the reduction in longitudinal RV strain. This situation — in which the RV transverse strain seems to compensate for the reduction in RV longitudinal strain — is similar to the situation of patients with systemic RV in whom a 'shift' from longitudinal to transverse and circumferential RV function has been observed [21,22].

Our report also focuses on the role of RV apical deformation in Eisenmenger syndrome, which was clearly different to controls. The role of apical longitudinal motion and apical traction has been recently described [23]. Apical traction — visually defined by the cardiac apex being pulled toward the left ventricle — has been associated with death or transplantation [23]. The finding of apical traction of the right ventricle towards the left ventricle in this study can be compared to a reduction in apical RV longitudinal strain. Our patients with Eisenmenger syndrome, despite presenting with reduced RV longitudinal strain compared to controls, more frequently presented a predominant apical function. This might partially explain the classically described improved survival in such patients.

Study limitations

This was a case-control two-centre study. Unfortunately, two different ultrasound machines and probes were used, limiting us to the use of vendor-independent speckle-tracking software with its own limitations [24]. Our cohort of patients was relatively small. Patients with complex cardiac anatomy, such as those with systemic right ventricles or univentricular physiology, were excluded from this study, given the difficulty in interpreting speckle-tracking imaging data in such patients. The intra-operator variability for RV strain was acceptable, however, as the same observer analysed the data, no conclusion can be drawn regarding

the overall feasibility and inter-operator variability of RV free-wall transverse strain.

Using 2D speckle-tracking analysis, only one view of the right ventricle was studied — the RV lateral wall, as assessed by the apical view — given the difficulties of assessing and interpreting other RV views. Despite this spatial limitation, 2D speckle-tracking of the right ventricle has been correlated with cardiac magnetic resonance data and associated with outcomes in patients with pulmonary hypertension [12,25,26]. Although deformation of the right heart occurs in three dimensions, circumferential strain could not be assessed in our cohort, due to technical limitations inherent in our adult population. In the future, three-dimensional speckle-tracking imaging of the right ventricle will probably provide a better understanding of RV adaptation [27,28].

Conclusion

In our population with Eisenmenger syndrome, differences in RV and LV strain were observed in comparison with the control population. Patients with Eisenmenger syndrome presented with reduced global LV longitudinal strain and RV free-wall longitudinal and transverse strain. The right ventricle of patients with Eisenmenger syndrome also frequently present a special feature — an increased apical deformation — as assessed by longitudinal and transverse strain. There was also evidence for LV longitudinal function impairment in patients with post-tricuspid shunt, but increased RV transverse strain. This single cardiac remodelling observed in patients with Eisenmenger syndrome might be related to favourable outcomes.

Sources of funding

The software Tomtec Cardiac Performance Analysis (TomTec Imaging Syststems GmbH, Germany) was funded by the Call Offer ''Innovation'' 2014 of the Nice University Hospital (AO2I CHU de Nice).

Disclosure of interest

The authors declare that they have no competing interest.

References

[1] Hoeper MM, Bogaard HJ, Condliffe R, et al. Definitions and diagnosis of pulmonary hypertension. J Am Coll Cardiol 2013;62:D42—50.
[2] Simonneau G, Gatzoulis MA, Adatia I, et al. Updated clinical classification of pulmonary hypertension. J Am Coll Cardiol 2013;62:D34—41.
[3] Hopkins WE, Ochoa LL, Richardson GW, Trulock EP. Comparison of the hemodynamics and survival of adults with severe primary pulmonary hypertension or Eisenmenger syndrome. J Heart Lung Transplant 1996;15:100—5.
[4] van Wolferen SA, Marcus JT, Boonstra A, et al. Prognostic value of right ventricular mass, volume, and function in idiopathic pulmonary arterial hypertension. Eur Heart J 2007;28:1250—7.
[5] Ghio S, Klersy C, Magrini G, et al. Prognostic relevance of the echocardiographic assessment of right ventricular function in patients with idiopathic pulmonary arterial hypertension. Int J Cardiol 2010;140:272—8.
[6] D'Alonzo GE, Barst RJ, Ayres SM, et al. Survival in patients with primary pulmonary hypertension. Results from a national prospective registry. Ann Intern Med 1991;115:343—9.
[7] Moceri P, Dimopoulos K, Liodakis E, et al. Echocardiographic predictors of outcome in eisenmenger syndrome. Circulation 2012;126:1461—8.
[8] Raymond RJ, Hinderliter AL, Willis PW, et al. Echocardiographic predictors of adverse outcomes in primary pulmonary hypertension. J Am Coll Cardiol 2002;39:1214—9.
[9] Moceri P, Kempny A, Liodakis E, et al. Physiological differences between various types of Eisenmenger syndrome and relation to outcome. Int J Cardiol 2015;179:455—60.
[10] Pirat B, McCulloch ML, Zoghbi WA. Evaluation of global and regional right ventricular systolic function in patients with pulmonary hypertension using a novel speckle tracking method. Am J Cardiol 2006;98:699—704.
[11] Hardegree EL, Sachdev A, Villarraga HR, et al. Role of serial quantitative assessment of right ventricular function by strain in pulmonary arterial hypertension. Am J Cardiol 2013;111:143—8.
[12] Motoji Y, Tanaka H, Fukuda Y, et al. Efficacy of right ventricular free-wall longitudinal speckle-tracking strain for predicting long-term outcome in patients with pulmonary hypertension. Circ J 2013;77:756—63.
[13] Fine NM, Chen L, Bastiansen PM, et al. Outcome prediction by quantitative right ventricular function assessment in 575 subjects evaluated for pulmonary hypertension. Circ Cardiovasc Imaging 2013;6:711—21.
[14] Rudski LG, Lai WW, Afilalo J, et al. Guidelines for the echocardiographic assessment of the right heart in adults: a report from the American Society of Echocardiography endorsed by the European Association of Echocardiography, a registered branch of the European Society of Cardiology, and the Canadian Society of Echocardiography. J Am Soc Echocardiogr 2010;23:685—713 [quiz 86—8].
[15] Douglas PS, DeCara JM, Devereux RB, et al. Echocardiographic imaging in clinical trials: American Society of Echocardiography Standards for echocardiography core laboratories: endorsed by the American College of Cardiology Foundation. J Am Soc Echocardiogr 2009;22:755—65.
[16] Lang RM, Badano LP, Mor-Avi V, et al. Recommendations for cardiac chamber quantification by echocardiography in adults: an update from the American Society of Echocardiography and the European Association of Cardiovascular Imaging. J Am Soc Echocardiogr 2015;28:1e14—39e14.
[17] Hardegree EL, Sachdev A, Fenstad ER, et al. Impaired left ventricular mechanics in pulmonary arterial hypertension: identification of a cohort at high risk. Circ Heart Fail 2013;6:748—55.
[18] Hopkins WE, Waggoner AD. Severe pulmonary hypertension without right ventricular failure: the unique hearts of patients with Eisenmenger syndrome. Am J Cardiol 2002;89:34—8.
[19] Van De Bruaene A, De Meester P, Voigt JU, et al. Right ventricular function in patients with Eisenmenger syndrome. Am J Cardiol 2012;109:1206—11.
[20] Moceri P, Bouvier P, Li W, et al. Survival advantage of Eisenmenger syndrome patients: the role of right ventricular transverse strain. Arch Cardiovasc Dis Suppl 2015;7:93, http://dx.doi.org/10.1016/S878-6480(15)71751-9 [abstract 0418].
[21] Pettersen E, Helle-Valle T, Edvardsen T, et al. Contraction pattern of the systemic right ventricle shift from longitudinal to circumferential shortening and absent global ventricular torsion. J Am Coll Cardiol 2007;49:2450—6.

[22] Di Salvo G, Pacileo G, Rea A, et al. Transverse strain predicts exercise capacity in systemic right ventricle patients. Int J Cardiol 2010;145:193—6.
[23] Unlu S, Farsalinos K, Ameloot K, et al. Apical traction: a novel visual echocardiographic parameter to predict survival in patients with pulmonary hypertension. Eur Heart J Cardiovasc Imaging 2015, http://dx.doi.org/10.1093/ehjci/jev131 [Epub ahead of print].
[24] Nagata Y, Takeuchi M, Mizukoshi K, et al. Intervendor variability of two-dimensional strain using vendor-specific and vendor-independent software. J Am Soc Echocardiogr 2015;28:630—41.
[25] Fukuda Y, Tanaka H, Sugiyama D, et al. Utility of right ventricular free wall speckle-tracking strain for evaluation of right ventricular performance in patients with pulmonary hypertension. J Am Soc Echocardiogr 2011;24:1101—8.
[26] Focardi M, Cameli M, Carbone SF, et al. Traditional and innovative echocardiographic parameters for the analysis of right ventricular performance in comparison with cardiac magnetic resonance. Eur Heart J Cardiovasc Imaging 2015;16:47—52.
[27] Addetia K, Maffessanti F, Yamat M, et al. Three-dimensional echocardiography-based analysis of right ventricular shape in pulmonary arterial hypertension. Eur Heart J Cardiovasc Imaging 2015, http://dx.doi.org/10.1093/ehjci/jev171 [Epub ahead of print].
[28] Smith BC, Dobson G, Dawson D, Charalampopoulos A, Grapsa J, Nihoyannopoulos P. Three-dimensional speckle tracking of the right ventricle: toward optimal quantification of right ventricular dysfunction in pulmonary hypertension. J Am Coll Cardiol 2014;64:41—51.